Light Metals 2012 *Edited by: Carlos E. Suarez*
TMS (The Minerals, Metals & Materials Society), 2012

Light Metals 2012

ALUMINUM ALLOYS: Fabrication, Characterization and Applications

Solutioning and Aging Behaviours

SESSION CHAIR

Tongguang Zhai
University of Kentucky
Lexington, Kentucky, USA

Light Metals 2012 *Edited by: Carlos E. Suarez*
TMS (The Minerals, Metals & Materials Society), 2012

THE ROLE OF CO-CLUSTERS IN THE ARTIFICIAL AGING OF AA6061 AND AA6060

Stefan Pogatscher[1], Helmut Antrekowitsch[1], Thomas Ebner[2], Peter J. Uggowitzer[3]
[1]Institute of Nonferrous Metallurgy, Montanuniversitaet Leoben, Franz-Josef-Strasse 18, 8700 Leoben, Austria
[2]AMAG Rolling GmbH, Postfach 32, 5282 Ranshofen, Austria
[3]Laboratory of Metal Physics and Technology, Department of Materials, ETH Zurich, Wolfgang-Pauli-Strasse 10, 8093 Zurich, Switzerland

Keywords: aluminum alloys, aging, precipitation, vacancies, phase transformation kinetics

Abstract

In this study the role of Mg,Si-co-clusters formed during long-term natural aging on the artificial aging behavior was investigated by hardness measurements for the alloys AA6061 and AA6060. It was found that kinetics and age hardening response of artificial aging at common temperatures (e.g. 170 °C) are lowered by a strong presence of co-clusters, but enhanced at high temperatures (e.g. 250 °C) for AA6061. Co-cluster formation in the alloy AA6060 increases the age hardening response at 170 °C, but barely influences kinetics in both temperature regions. The co-cluster dissolution was analyzed by a model based on temperature dependent reversion of the hardness, which showed similar activation energies for both alloys. It is supposed that the different behavior of the alloys AA6061 and AA6060 can be explained by solute-vacancy interactions.

Introduction

Nowadays Al-Mg-Si alloys are the commercially most frequently used group of age hardenable aluminum alloys [1]. Although they were developed 85 years ago, several aging phenomena are still poorly understood. This arises from the limits of available experimental methods [2] and the complexity of early stage precipitation reactions in this alloy system. Especially the influence of natural pre-aging on artificial aging, which depends on the type of Al-Mg-Si alloy and the temperature where artificial aging is performed [3], is not fully resolved even though it has been investigated over the last 70 years [2]. The alloys AA6061 and AA6060 are important members in the family of Al-Mg-Si alloys and mark two extreme cases concerning the influence of natural pre-aging [4]. Alloys with higher alloying content such as AA6061 are used for applications that require higher strength such as construction, automotive engineering, shipbuilding and the aircraft industry. For these alloys a strong adverse influence of natural pre-aging on the precipitation kinetics and the hardening response at common artificial aging temperatures (e.g. 170 °C) has been reported [5-8]. Further it has been reported recently that kinetics and age hardening response of AA6061 can also be enhanced by natural pre-aging, when artificial aging is performed at unconventional high temperatures (e.g. 250 °C) [3]. Lean alloys such as AA6060 provide a medium strength and are often used for extrusions in transportation [4]. In contrast to rich alloys a positive influence of natural pre-aging has been found at common artificial aging temperatures [8,9].

Beside the fundamental aspect of understanding the mechanisms responsible for the ambiguous influence of natural pre-aging, the negative effect in rich alloys is of considerable industrial importance because the production of many heat-treated semi-finished products is affected by logistically unavoidable natural pre-aging [4]. Furthermore, the use of such alloys for automotive outer panel applications is restricted by the sluggish kinetics after intermediate natural aging. This led to the development of numerous heat treatments strategies to minimize the negative effect of natural pre-aging [10-15]. The industrial importance of the negative effect might be the reason that rich alloys have been extensively studied at common artificial aging temperatures, while lean alloys and unconventional artificial temperatures have been barely investigated. For an appropriate examination of these two previously untended issues the precipitation sequence of Al-Mg-Si alloys should be addressed first [16]:

SSSSS → Individual clusters → Co-clusters → GP-I zones → β″→ β′ and others → β

Note that this general sequence is not without controversy in the early stages, can differ with the alloy composition, and is only valid during linear heating. After the first stages including individual solute clustering of Si and Mg and cluster dissolution reactions, Mg,Si-co-clusters are formed from the super-saturated solid solution (SSSS) [16]. Co-clusters [2,9,16,17-19] were also found after long-term room temperature exposure, whereat Banhart *et al.* [1] recently reported that natural aging of Al-Mg-Si alloys is a rather complex process taking place in several individual stages. Since the notation of the finally formed clusters is not consistent in the literature (co-clusters are termed as both initial-β″ [20] and GP-zones [21]) in this work the term co-cluster is only used for clusters formed after long-term natural aging. Consecutively formed GP-I zones [22-24] are thermally more stable, contain more solute atoms, and are most often found to be spherical, with a typical size of 1 to 3 nm [25]. At peak aged states needle-like monoclinic β″ (Mg_5Si_6) precipitates were found to be responsible for the major hardness increase [25,26]. For overaged microstructures various hexagonal rod-shaped phases [16,21,22,27-29] have been reported (β′ and others). The equilibrium phase is the platelet-like β precipitate (Mg_2Si) [16,20,21,30]. In the past many researchers argued on the negative influence of natural pre-aging at common artificial aging temperatures more or less addressing the role of co-clusters during artificial aging. Ried *et al.* [8] thought that natural aging reduces the vacancy concentration and solute super-saturation (due to the formation of co-clusters), which should rise the critical nucleation size for β″ [31]. Murayama *et al.* [18] expected that co-clusters, which form during room temperature storage, are too small to act as nucleation sites for β″ and would be completely reverted at common artificial aging temperatures. Resent results indicate that artificial aging kinetics of AA6061 is controlled via the concentration of mobile vacancies, which is determined by a temperature-dependent dissolution of co-clusters associated with the release of imprisoned quenched-in vacancies. Due to a very slow co-cluster dissolution at low temperatures the precipitation process is strongly retarded at common artificial aging temperatures and enhanced at high artificial aging temperatures [3]. The positive effect has not been investigated

comprehensively, but Chang *et al.* [9] assumed that in lean alloys a different nature of co-clusters might exist, which dissolve very slowly and could serve as nuclei for subsequent phases. However, the picture of the role of co-clusters during artificial aging at different temperatures for various Al-Mg-Si alloys is far from complete. Thus, the present work was performed to investigate the artificial aging behavior at common and high temperatures of two principal Al-Mg-Si alloys especially focusing on the role of co-clusters.

Experimental Methods

The alloy AA6061 was supplied by AMAG Rolling and the alloy AA6060 was provided by Light Metals Technologies Ranshofen. Their composition is given in Table I.

Table I. Composition of alloy AA6060 and AA6061

Alloy \ wt%	Si	Fe	Cu	Mn	Mg	Cr
AA6060	0.41	0.17	-	-	0.43	-
AA6061	0.60	0.52	0.22	0.11	0.82	0.15

Solution heat treatment was performed in a circulating air furnace (Nabertherm N60/85 SHA) at 570 °C for 20 min. Specimens were then heat treated according the time-temperature sequences described in Figure 1. Quenching was carried out in water at RT, followed by natural pre-aging for $1.2 \cdot 10^2$ s (B1) and $1.2 \cdot 10^6$ s (B2) at 25 °C. In order to achieve a good temperature accuracy during artificial aging, an oil bath (LAUDA Proline P 26) with an integrated basin filled with a low-melting alloy as a high performance heat transfer medium (Bi57Sn43) was used. Samples were positioned in a cage near a platinum thermometer (Pt100), which facilitated a temperature accuracy of ± 0.1 °C.

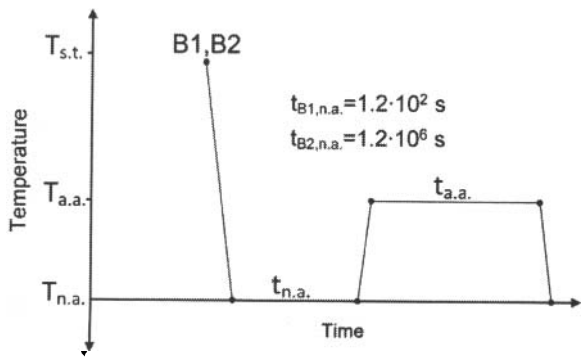

Figure 1. Heat treatment procedure

Brinell hardness measurements were performed in an EMCO-Test M4 unit. For the alloy AA6061 HBW 2.5/62.5 was used. Especially for the lower range of the hardness of the softer alloy AA6060 this method is not optimal. Therefore HBW 2.5/31.25, which facilitated a more accurate measurement in terms of deviation of the measured hardness values, was used. Note that hardness values measured with different methods cannot be exactly converted into each other in principal. But for the present study it was proven experimentally that both values do not differ strongly in the investigated range and can therefore be roughly compared.

Experimental Results

Natural Aging

Hardness curves for natural aging at 25 °C of AA6060 and AA6061 are shown in Figure 2. After a slow initial change and a rapid hardness increase a nearly constant value of 39.2 HBW 2.5/31.25 was reached for AA6060 (Figure 2a). AA6061 exhibited the same three stage behavior resulting in a nearly constant hardness value of 73 HBW 2.5/62.5 (Figure 2b). The natural aging kinetics of AA6060 is only slightly slower than for AA6061, but the total increase of the hardness is much lower for the alloy AA6060.

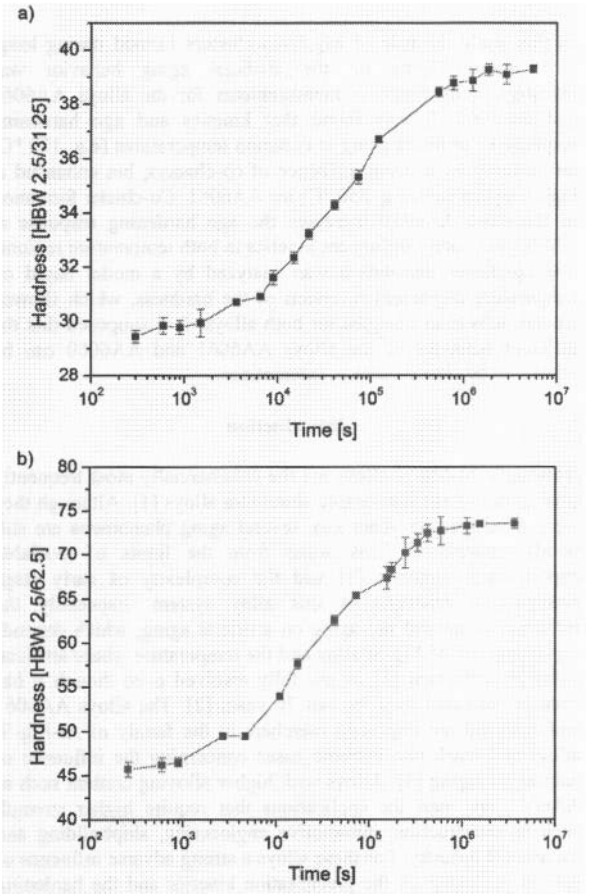

Figure 2. Hardness curve for natural aging at 25 °C of a) AA6060 and b) AA6061

Artificial Aging

Hardness curves obtained by the artificial aging procedures B1 and B2 at 170 °C are shown for AA6060 and AA6061 in Figure 3. In order to help the reader, additionally the hardness measured after long-term natural aging (n.a.) is plotted. Examining alloy AA6060, the intermediate natural aging (B2) shifted the hardness curve to higher values, whereby the contribution of co-clusters to the hardness seems to be constant over a long aging time and no significant reversion was observed (Figure 3a). Kinetics was not affected by long-term natural pre-aging (B2) and has been found to be similar but very slow for B1 and B2. The alloy AA6061 exhibited a totally different behavior (Figure 3b). Artificial aging

directly after quenching (B1) resulted in very rapid kinetics and high peak hardness. For B2, kinetics was found to be strongly retarded and nearly as slow as for the alloy AA6060. Furthermore, the peak hardness of B2 is lower than for B1. Similar to AA6060 no observable reversion of co-clusters took place.

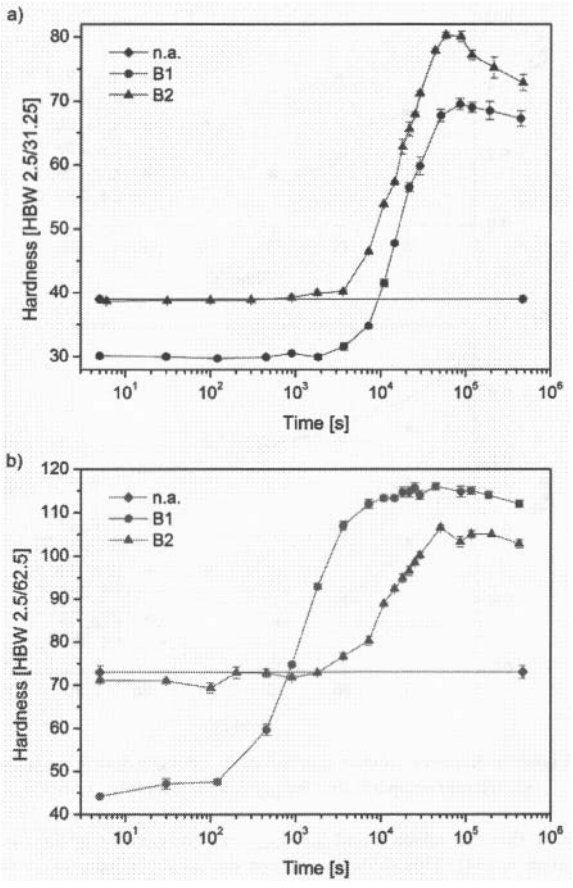

Figure 3. Hardness curves for artificial aging procedures B1 and B2 at 170 °C for (a) AA6060 and (b) AA6061

The hardening behavior of the two alloys applying procedure B1 and B2 at 250 °C artificial aging temperature is shown in Figure 4. Beside a rapid reversion of the hardness, reached after natural aging and a slightly higher peak hardness for B2, both heat treatment procedures exhibited similar kinetics for the alloy AA6060 (Figure 4a). Compared to artificial aging at 170 °C faster kinetics has been found for B1 and B2, so that the initial period till the first hardness increase occurred, reduced from ~ $3 \cdot 10^3$ s to ~ 10^2 s and the time to peak hardness decreased from ~ $7 \cdot 10^4$ s to ~ $3 \cdot 10^3$ s. For the alloy AA6061 a different behavior has been found (Figure 4b). Beside a rapid reversion, procedure B2 showed accelerated aging kinetics and significant higher peak hardness than B1. Compared to artificial aging at 170 °C extremely enhanced kinetics has been found for B2, so that the initial period till the first hardness increase occurred, reduced from ~ $2 \cdot 10^3$ s to ~$2 \cdot 10^1$ s and the time to peak hardness decreased from ~ $1 \cdot 10^5$ s to ~ $9 \cdot 10^2$ s. Interestingly, B1 revealed nearly the same initial period till the first hardness increase occurred (~ 10^2 s) at both temperatures, while the time to peak hardness decreased from ~ $3 \cdot 10^4$ s to ~ $3 \cdot 10^3$ s.

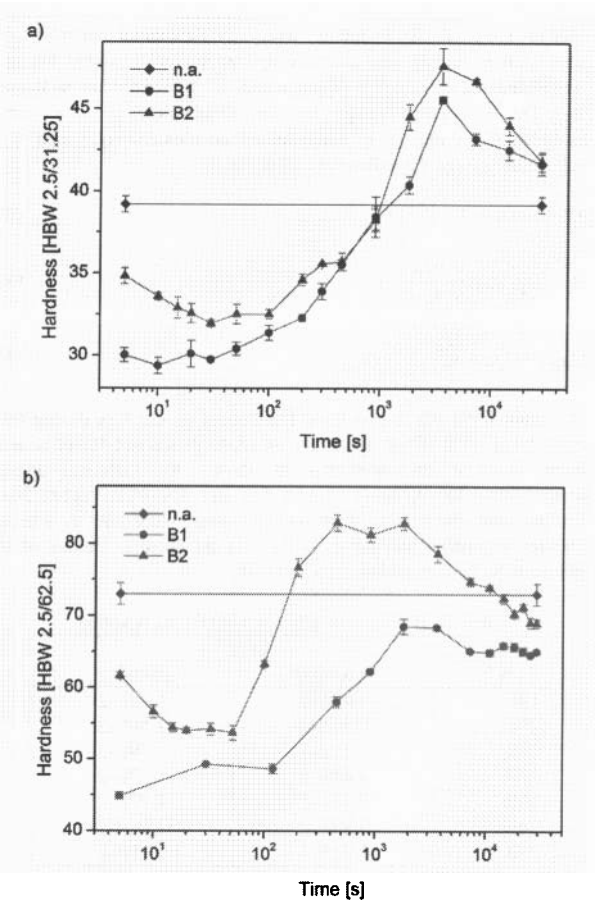

Figure 4. Hardness curves for artificial aging procedures B1 and B2 at 250 °C for (a) AA6060 and (b) AA6061

Co-cluster Dissolution

The reversion of the hardness is a good indicator for the dissolution of co-clusters formed during long-term natural aging, which can be analyzed by a simple model already used for this purpose in [3]. Its basic assumptions have to be considered and should be briefly recapitulated. The hardness is supposed to be proportional to the contribution of co-clusters, treated as shearable obstacles [32-34], to the yield strength. Furthermore, the slightly increasing solution strengthening is neglected. Accepting this, a relationship between the relative volume fraction of co-clusters ($f_r^{n.a.}$) and the hardness during early stages of the reversion, where the contribution of aging is negligible, can be express by Eq. (1). The hardness after long-term natural aging ($H_{n.a.}$) was set to 39.2 HWB 2.5/31.25 for AA6060 and to 73 HBW 2.5/62.5 for AA6061. For AA6060 the as-quenched hardness ($H_{a.q.}$) was found to be 29 HBW 2.5/31.25 and for AA6061 a value of 43 HBW 2.5/62.5 was measured.

$$\sqrt{f_r^{n.a.}} \propto \frac{H - H_{a.q.}}{H_{n.a.} - H_{a.q.}} \qquad (1)$$

The time-dependence of $f_r^{n.a.}$ during reversion can be described by Eq. (2), which basically results of a mathematical model for a diffusion-controlled solution of a second phase in an infinite matrix [34]. B is a factor with an Arrhenius temperature dependence (Eq. 3), characterized by the activation energy for the dissolution of co-clusters ($Q_{diss.}$) and the pre-exponential factor B_0. The activation energy for the dissolution of co-clusters includes the enthalpy of solution of co-clusters (Q_s) and the activation energy for diffusion (Q_d) (Eq. 4).

$$f_r^{n.a.} = (1 - B \cdot t^{0.5})^3 \tag{2}$$

$$B = B_0 \cdot exp\left(\frac{-Q_{diss.}}{k \cdot T}\right) \tag{3}$$

$$Q_{diss} = Q_s + \frac{Q_d}{2} \tag{4}$$

In Figure 5 the relative volume fraction of co-clusters during the early stage of artificial aging according to procedure B2 obtained from hardness measurements is shown for different aging temperatures for AA6060 (Figure 5a) and AA6061 (Figure 5b). Furthermore, the results of fitting the experimental data by a least squares algorithm according to Eq. (2) are shown. Values of B obtained by fitting are listed in Table II.

Table II. B-values of alloy AA6060 and AA6061

	B [$s^{-0.5}$]	
T [°C]	AA6060	AA6061
190	1.42E-2	1.24E-2
200	1.81E-2	2.54E-2
210	3.13E-2	3.39E-2
220	4.41E-2	5.07E-2
230	7.47E-2	7.77E-2
240	9.84E-2	1.01E-1
250	1.31E-1	1.28E-1

The activation energy for the dissolution of co-clusters and the pre-exponential factor B_0 can be determined by an Arrhenius plot of Eq. (3) (Figure 6). For AA6060 the value for $Q_{diss.}$ was found to be 79 kJmol^{-1} and B_0 revealed a value of $9.8 \cdot 10^{-6}$ $s^{-0.5}$.The alloy AA6061 showed insignificantly lower values for the activation energy (77 kJmol^{-1}) and B_0 ($6.6 \cdot 10^{-6}$ $s^{-0.5}$).

Discussion

The present study reveals a totally different influence of the co-cluster formation during long-term natural aging on subsequent artificial aging at common (e.g. 170 °C) and high temperatures (e.g. 250°C) for the alloys AA6060 and AA6061. A significant increase of the hardening response, but no influence on kinetics was observed for AA6060 at 170 °C (Figure 3a). At 250 °C the long-term natural aging showed a rather small influence, excepting the dissolution of co-clusters at the very beginning of artificial aging (Figure 4a). For AA6061 kinetics and age hardening response of artificial aging at 170 °C are strongly lowered by the presence of co-clusters, while both are significantly enhanced at 250 °C (Figure 3b, Figure 4b). Interestingly, the analysis of the dissolution of co-clusters during artificial aging revealed a similar behavior for both alloys (Figure 5, Figure 6).

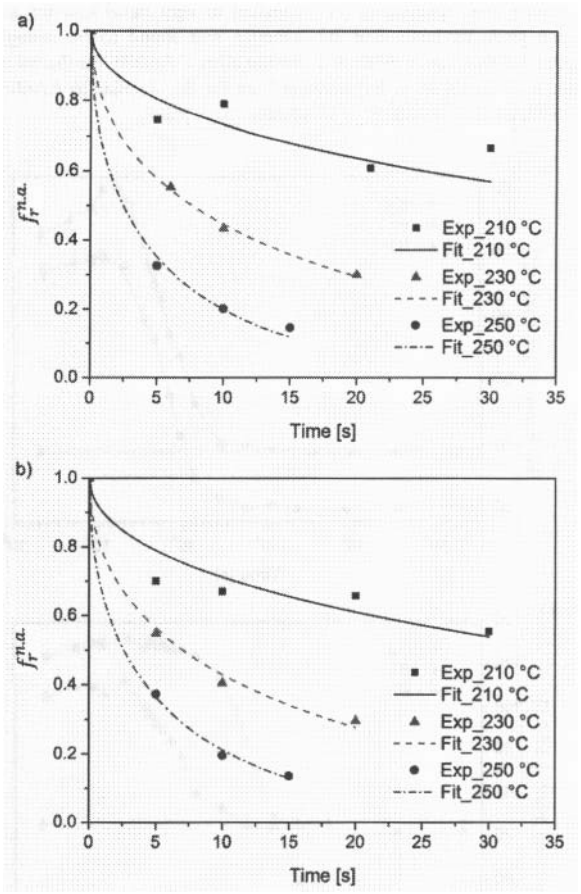

Figure 5. Relative volume fraction of co-clusters during reversion at different temperatures for (a) AA6060 and (b) AA6061

Note that the values found for $Q_{diss.}$ are comparable to the value given in [34]. This findings contrast the idea of Chang *et al.* [9], who speculated that a different nature of co-clusters exists in lean alloys, dissolving very slowly and serving as nuclei. Instead, we believe that the rather complex effects of long-term natural aging of different Al-Mg-Si alloys can be explained on the basis of quenched-in vacancies, which has been shown to be necessary for the nucleation of β'' [35] in Al-Mg-Si alloys. Therefore two principal assumptions concerning vacancy-solute interactions have to be made:

i) Co-clusters can contain and release quenched-in vacancies.
ii) The mobility of quenched-in vacancies depends on their interaction with solute atoms.

Assumption (i) has been previously described in [3] as the so-called 'vacancy prison mechanism' and explains the influence of long-term natural pre-aging on artificial aging of AA6061 via the concentration of mobile vacancies, which is determined by a temperature-dependent dissolution of co-clusters associated with the release of imprisoned quenched-in vacancies. Assumption (ii) is somehow comparable to the 'temporarily stabilization' of vacancies used in [3] explaining a retarded annihilation. For the current discussion this concept is used in a more general way.

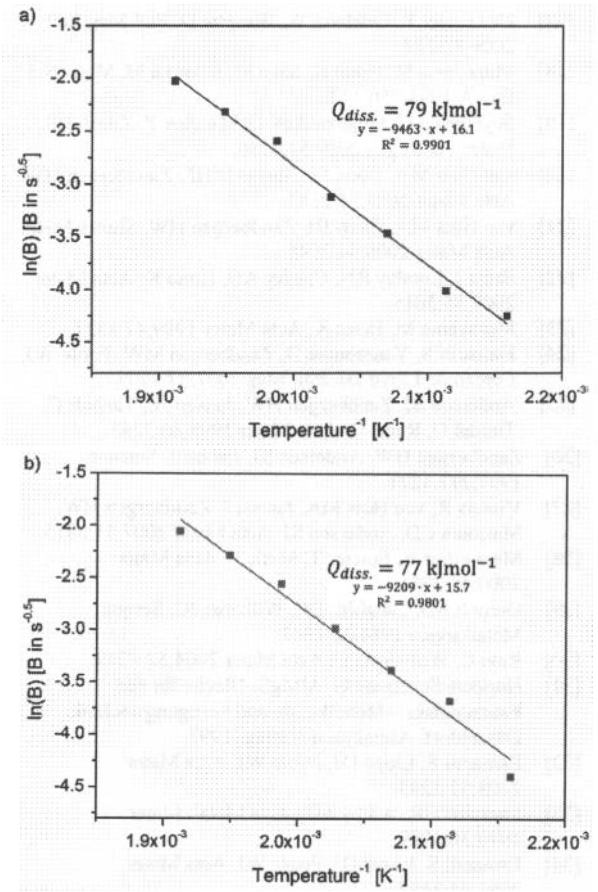

Figure 6. Arrhenius plot of Eq. (3) for (a) AA6060 and (b) AA6061

Although the exact binding energy of Mg and Si with vacancies is still under discussion [36] an association tendency of vacancies with Mg atoms during natural aging has been shown by positron annihilation lifetime spectroscopy (PALS) [19,37,38]. Furthermore, it has been found that the annihilation of quenched-in vacancies is prevented by Mg in aluminum at room temperature and delayed at temperatures above 100 °C [39,40]. In general lattice sites next to attractive solute atoms are energetically preferential for quenched-in vacancies whereby the formation of vacancy-solute pairs or complexes is promoted [41]. Note that also in the equilibrium state solute-vacancy complexes, at least as pairs, exist if attractive interactions to solute atoms are present [42]. Barnhart *et al.*[1,2] reported that an association tendency of vacancies and solute within the first few minutes of natural aging or even during quenching is very likely in Al-Mg-Si alloys. In such constellation, solute atoms can either change their lattice sites with the vacancy, or matrix atoms jump into the vacancy around the solute atom, which leads to a preferential movement of the vacancy around the solute atom. Compared to pure metals, jumps are therefore not longer random. From this non-random walk it is evident that the statistical length which a quenched-in vacancy can move to an annihilation sink is reduced, and annihilation is retarded. Consequently, annihilation depends on the chemical composition, assuming a similar number density of annihilation sites such as free surface, grain boundaries and dislocations [43].

AA6060

Intermediate long-term natural aging (B2) shifted the hardness curve, obtained by artificial aging at 170 °C, to higher values (Figure 3a). This can be explained by the contribution of co-clusters, slowly dissolving at this temperature. Note that the difference in the hardness is constant over a long period and reduces just in late stages of aging. Due to slow but similar kinetics found for B1 and B2 (Figure 3a), the precipitation process during artificial aging is assumed to be controlled by the same mechanisms. For artificial aging at 250 °C a rapid reversion took place for B2. Thereafter, both heat treatment procedures exhibited similar kinetics and just small differences in the hardness (Figure 4a). The fact that the precipitation process including nucleation (simplified here as the initial period until the hardness starts to increase) and growth is accelerated with rising temperature can be easily explained by thermally activated diffusion (increasing equilibrium concentration of vacancies) in a super-saturated solid solution with large undercooling [44]. In contrast to AA6061 [3] it is believed that co-clusters in AA6060 contain no vacancies which can be released during B2. Furthermore, a rapid annihilation of quenched-in vacancies during quenching and initial stages of artificial aging according to B1 is supposed. Both can be explained by a low concentration of solute in lean alloys, which provide a low number density of preferential sites for vacancies next to attractive solute atoms (assumption (ii)). Quenched-in vacancies might anneal out during natural aging for B2 or before the critical size for the nucleation of β″ is reached in the case of B1. Conclusively, the precipitation process in AA6060 is governed by the same concentration of vacancies near the equilibrium for B1 and B2, which is in good accordance with thermally activated diffusion controlling the precipitation reaction.

AA6061

The influence of natural aging on artificial aging of AA6061 has been already explained in [3] by the temperature-dependent release of imprisoned quenched-in vacancies from co-clusters. Anyhow, it is necessary to make some remarks to get a complete picture of Al-Mg-Si alloys including lean alloy. For heat treatment procedure B2, co-clusters act as 'prisons' for quenched-in vacancies at 170 °C artificial aging temperature and therefore strongly retard the precipitation process. Note that kinetics is just slightly faster as for B1 and B2 of AA6060 (Figure 3). At 250 °C imprisoned quenched-in vacancies are released from dissolving co-clusters and precipitation kinetics is enhanced. Note that for B2, kinetics (especially the nucleation time) is much stronger accelerated than for the alloy AA6060 by rising the temperature. The fast kinetics found at 170 °C for AA6061 according to B1 has been attributed to a high concentration of quenched-in vacancies [3]. Because they are essential for the nucleation of β″[35], the critical size of nuclei must be reached before most quenched-in vacancies have been annealed out. This can be easily understood applying assumption (ii) to rich alloys with a high number density of preferential lattice sites for vacancies. A further indication of the importance of quenched-in vacancies during initial stages at 170 °C for B1 is that the nucleation time does not significantly differ for B1 at 170 °C and 250 °C and is in the same range as for AA6060 at 250 °C. A decreasing time to peak hardness with

rising temperature for B1 can be explained by the fact that thermally activated diffusion is getting dominant after annihilation has finished.

Conclusions

The objective of this study was to shed more light on the influence of co-clusters formed during long-term natural aging on artificial aging at common and high temperatures for the two principal types of Al-Mg-Si alloys.

In lean alloys, artificial aging is controlled by thermally activated diffusion, independently of the thermal history. After natural pre-aging, slowly dissolving vacancy free co-clusters contribute to the hardness at common artificial aging temperatures which has been previously called the 'positive' influence.

In the case of rich alloys and natural pre-aging, artificial aging is controlled by a temperature dependent dissolution of co-clusters and a concurrent release of imprisoned vacancies [3]. The enhanced kinetics at common artificial aging temperatures for direct aging can be explained by quenched-in vacancies, which contribute to the nucleation before they anneal out.

Acknowledgment

The authors gratefully thank the people at AMAG Rolling for the fruitful discussion and providing the alloys. Furthermore we want to thank the Austrian Research Promotion Agency (FFG) and AMAG Rolling for the financial support of this work.

References

[1] Banhart J, Lay MDH, Chang CST, Hill AJ. Phys Rev B 2011;83:art. no. 014101.
[2] Banhart J, Chang CST, Liang ZQ, Wanderka N, Lay MDH, Hill AJ. Advanced Engineering Materials 2010;12:559.
[3] Pogatscher S, Antrekowitsch H, Leitner H, Ebner T, Uggowitzer PJ. Acta Mater 2011;59:3352.
[4] Ostermann F. Anwendungstechnologie Aluminium. Berlin Heidelberg New York: Springer-Verlag; 2007.
[5] Brenner P, Kostron H. Z Metall 1939;4:89.
[6] Borchers H, Kainz M. Metall 1963;17:400.
[7] Kovacs I, Nagy E, Lendvai J. Acta Metall 1972;20:975.
[8] Ried A, Schwellinger P, Bichsel H. Aluminium 1977;53:595.
[9] Chang CST, Wieler I, Wanderka N, Banhart J. Ultramicroscopy 2009;109:585.
[10] Zhuang L, Janse JE, De Smet P, Chen JH, Zandbergen HW. In: Das SK, Kaufman JG, Lienert TJ, editors. Aluminum 2001. Warrendale (PA): TMS; 2001. p. 77.
[11] Roset J, Stene T, Saeter JA, Reiso O. Mater Sci Forum 2006;519-521:239.
[12] Bryant JD. Metall Mater Trans A 1999;30:1999.
[13] Saga M, Sasaki Y, Kikuchi M, Yan Z, Matsuo M. Aluminium Alloys: Their Physical and Mechanical Properties 1996;217:821.
[14] Slámova M, Janecek M, Cieslar M, Šíma V. Mater Sci Forum 2007;567-568:333.
[15] Ou BL, Shen CH. Scand J Metall 2005;34:318.
[16] Edwards GA, Stiller K, Dunlop GL, Couper MJ. Acta Mater 1998;46:3893.
[17] De Geuser F, Lefebvre W, Blavette D. Phil Mag Lett 2006;86:227.
[18] Murayama M, Hono K, Saga M, Kikuchi M. Mater Sci Eng A 1998;250:127.
[19] Seyedrezai H, Grebennikov D, Mascher P, Zurob HS. Mater Sci Eng A 2009;525:186.
[20] van Huis MA, Chen JH, Sluiter MHF, Zandbergen HW. Acta Mater 2007;55:2183.
[21] van Huis MA, Chen JH, Zandbergen HW, Sluiter MHF. Acta Mater 2006;54:2945.
[22] Buha J, Lumley RN, Crosky AG, Hono K. Acta Mater 2007;55:3015.
[23] Murayama M, Hono K. Acta Mater 1999;47:1537.
[24] Esmaeili S, Vaumousse D, Zandbergen MW, Poole WJ, Cerezo A, Lloyd DJ. Phil Mag 2007;87:3797.
[25] Anderson SJ, Zandbergen HW, Jansen JE, Taeholt C, Tundal U, Reiso O. Acta Mater 1998;46:3283.
[26] Zandbergen HW, Andersen SJ, Jansen J. Science 1997;277:1221.
[27] Vissers R, van Huis MA, Jansen J, Zandbergen HW, Marioara CD, Andersen SJ. Acta Mater 2007;55:3815.
[28] Massardier V, Epicier T, Merle P. Acta Mater 2000;48:2911.
[29] Dumolt SD, Laughlin DE, Williams JC. Scripta Metallurgica 1984;18:1347.
[30] Ravi C, Wolverton C. Acta Mater 2004;52:4213.
[31] Huppert-Schemme G. AlMgSi-Bleche für den Fahrzeugbau – Metallkunde und Fertigungstechnik. Düsseldorf: Aluminium-Verlag; 1997.
[32] Esmaeili S, Lloyd DJ, Poole WJ. Acta Mater 2003;51:2243.
[33] Shercliff HR, Ashby MF. Acta Metall Mater 1990;38:1789.
[34] Esmaeili S, Lloyd DJ, Poole WJ. Acta Mater 2003;51:3467.
[35] Pogatscher S, Antrekowitsch H, Leitner H, Pöschmann D, Zhang Z, Uggowitzer PJ. Influence of Interrupted Quenching on Artificial Aging of Al-Mg-Si Alloys. to be published.
[36] Wolverton C. Acta Mater 2007;55:5867.
[37] Dupasquier A, Kögel G, Somoza A. Acta Mater 2004;52:4707.
[38] Buha J, Muramatsu T, Lumley RN, Crosky AG, Hillel AJ. Mater Forum 2004;28:1028.
[39] Panseri C, Federighi T, Ceresara S. Trans Metall Soc AIME 1963;227:1122.
[40] Panseri C, Gatto FG, Federighi T. Acta Metall 1958;6:198.
[41] Zurob HS, Seyedrezai H. Scr Mater 2009;61:141.
[42] Takamura J, Koike M, Furukawa K. J Nucl Mater 1978;69-70:738.
[43] Fischer FD, Svoboda J, Appel F, Kozeschnik E. Acta Mater 2011;59:3463.
[44] Liu F, Sommer F, Bos C, Mittemeijer EJ. International Materials Reviews 2007;52:193.